Proc. of the European Safety and Reliability Conference (ESREL 2026)
Edited by José C. Matos, Paulo B. Lourenço, Michael Beer, Daniel Oliveira,
Edoardo Patelli, Hélder S. Sousa, Rui A. Silva and Monica Santamaria
 Published by Research Publishing, Singapore.
doi: 10.3850/ESREL2026061419_esrel26-p26568-cd

Integrating Reliability Analysis and Sustainability Assessment – Illustrating the Potential by Comparison of Additive and Subtractive Manufactured Component Designs

Dshamil Efinger

Institute of Machine Components, University of Stuttgart, Germany.
E-mail: dshamil.efinger@ima.uni-stuttgart.de

Tim Prescher

Institute of Acoustics and Building Physics, University of Stuttgart, Germany.
E-mail: tim.prescher@iabp.uni-stuttgart.de

Stefan Albrecht

Fraunhofer Institute for Building Physics IBP, Stuttgart, Germany. E-mail: stefan.albrecht@ibp.fraunhofer.de

Martin Dazer

Institute of Machine Components, University of Stuttgart, Germany.
E-mail: martin.dazer@ima.uni-stuttgart.de

Service life and usage phase are central parameters in life cycle assessment (LCA), but numerical values are often based only on empirical values or estimates. This paper presents a simulation-based co-design of reliability and environmental sustainability for a dynamically loaded PA6-GF30 bracket, comparing additive manufacturing (AM) and milling from plate stock (CNC) under an equal-function constraint. It couples reliability-based design verification with global warming potential (GWP) evaluation and iteratively identifies levers where design optimization can reduce impacts without violating reliability targets. The verification chain comprises beam-theory pre-sizing, strength assessment based on VDI 2016, and finite-element analysis in ANSYS. Material behavior is modeled process specific anisotropic. Sustainability is quantified cradle-to-grave with GWP.
A baseline AM design requires increased section height and leg width to meet fatigue requirements, resulting in higher mass and – due to process-related factors – a substantially higher GWP than CNC. Based on the identified levers, function-preserving AM lightweight measures are applied retaining required product lifetime while lowering GWP. Finally, the AM bracket is not only lighter but also results in a lower GWP while maintaining the same reliability as the CNC variant.

Keywords: Reliability, Environmental Sustainability, Co-Design, Product Design, Global Warming Potential (GWP).

1. Motivation

The selection of manufacturing processes constrains product design and thereby influences product reliability and service life (Boothroyd et al. (2010)). Moreover, process selection can make an important contribution to achieving climate protection goals. Reducing greenhouse gas emissions in particular should be a priority in order to meet climate protection goals (Rockström et al. (2024)). Determining manufacturing routes with regard to environmental impacts can thus contribute to sustainability. The environmental impact of a product is assessed using a life cycle assessment (LCA). When conducting an LCA, the entire life cycle should be considered as far as possible. For functional products and products that are subject to mechanical force, the use phase is particularly important in the life cycle.

According to European Commission (2021) for an LCA the functional unit should define (i) the function provided (what); (ii) the extend of the function (how much); (iii) the expected level of quality (how well); (iv) the duration/life time of the product (how long). The information of "how well" and "how long" is often estimated and not specifically intended for LCA (Bongono et al. (2020)) (Pérez et al. (2024)).

Design for Reliability and testing can be used to engineer products in a targeted manner and to characterize their in-use lifetime. This enables to achieve and demonstrate the reliability requirements, while also providing the lifetime and performance data needed as important inputs for LCA.

In this study, a bracket produced via two different process routes (milling from plate stock and additive manufacturing) is being investigated. Reliability design and other boundary conditions ensures the functional equivalence of the variously manufactured brackets during their use phase. Furthermore, the brackets are evaluated in terms of their environmental impact. The findings from reliability assessment and LCA are used together to gain insight into how the product can be optimized for sustainability without compromising its reliability or functionality.

2. Methodical Approach

A reliability requirement is specified as a minimum reliability at a defined lifetime and must be demonstrated at a given confidence level (Bertsche and Dazer (2022)). The design of the bracket follows a multi-stage procedure as described in Section 4.

To quantify the environmental impacts of a product through its entire life cycle, an LCA is applied. The methodological framework of an LCA is defined according to DIN ISO 14040 (International Organization for Standardization (2006a)) and DIN ISO 14044 (International Organization for Standardization (2006b)). An LCA proceeds in four phases: (1) Definition of goal and scope; (2) life cycle inventory (LCI); (3) life cycle impact assessment (LCIA); (4) interpretation of the results. The impacts of global warming potential (GWP) were considered in this study. They are calculated using the EF3.1 impact assessment method, which is part of the Product Environmental Footprint (PEF) standard published by the European commission and is based on DIN ISO 14040.

The process comparison is based on an integrated reliability–LCA co-design framework that establishes comparability not through identical geometries, but through functional equivalence defined by explicit reliability requirements. Accordingly, the functional unit is defined as one bracket that, under an identical load spectrum and the same boundary conditions, is first subjected to a reliability-oriented preliminary design for each manufacturing route (milling from plate stock and additive manufacturing). Route-specific, material- and orientation-dependent strength and fatigue properties are considered to derive an initial reliability-compliant design space. The resulting functionally equivalent baseline geometries determine material demand, process energy, and process-induced uncertainties, and thus provide the consistent basis for the subsequent GWP assessment.

Based on the preliminary design, optimization levers for both objectives are then identified: reliability-relevant design parameters, critical stress and damage zones, and, from an LCA perspective, hotspot contributors along the respective process chains. These levers guide the joint optimization of process-specific product variants, which are numerically verified and re-evaluated in the GWP model. This yields reliability-equivalent designs with reduced GWP and enables a fair, application-oriented comparison of manufacturing routes.

3. Scenario and LCA Setup

The bracket is used to vertically transfer components with scratch-sensitive surfaces between two conveyor belts with an elevation offset in a material-handling system. During pickup on the lower conveyor, the bracket is translated upward with a uniform linear displacement within $1\,\mathrm{s}$ until the full payload of $10\,\mathrm{kg}$ is supported. Subsequently, the component is transported to the upper conveyor within $8\,\mathrm{s}$ along a prescribed trajectory with an associated kinematic profile; the acceleration follows a sinusoidal time history. Placement on the upper conveyor is performed by reversing the pickup sequence. The resulting load-time history and a schematic illustration of the transfer operation are shown in Figure 1. After completion of one transfer cycle, the bracket remains in a dwell phase for several minutes until the next component arrives.

Due to packaging constraints, the component interface region of the bracket is limited to a maximum width of $40\,\mathrm{mm}$ and must provide an opening diameter of at least $24\,\mathrm{mm}$. To enable component engagement, a frontal clearance opening of at least $10\,\mathrm{mm}$ is required. Load introduction from the component occurs via two locking pins located at $2/3$ of the leg length. The bracket is positioned and clamped within the linear actuator by means of planar locating surfaces in the rear section. The operating temperature range is 10–$30\,^{\circ}\mathrm{C}$; ambient humidity corresponds to typical indoor workplace conditions.

The bracket is required to achieve a B_5 life (survival probability of $95\,\%$) of $10{,}000$ load cycles at $90\,\%$ confidence level under the specified conditions. Over the target lifetime, the maximum permissible tip deflection under the maximum load is $5\,\mathrm{mm}$.

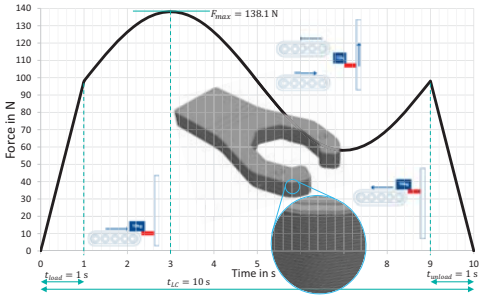

Fig. 1. Load scenario and AM model design.

Two manufacturing routes were examined. Since the bracket is intended for low-volume manufacturing and decentralized spare-part production, injection molding was not considered.

In the subtractive manufacturing route (CNC), plate stock is used as the starting material. After sawing to near-net shape with a machining allowance, the bracket is produced by milling on a computer numerical controlled milling machine.

For the additive manufacturing route (AM), filament serves as the feedstock and the bracket is fabricated layer-by-layer by fused filament fabrication (FFF). Manufacturing is conducted on a miniFactory Ultra 3D Printing System featuring an enclosed, heated build chamber and an integrated climate chamber for filament preconditioning. To ensure high mechanical performance of the FFF-fabricated brackets, the filament is dried prior to processing according to the material supplier's specifications.

Both manufacturing routes employ materials with identical upstream supply chains. Further details on material selection and anisotropic material behavior are provided in Section 4.

The process chains for brackets produced by both routes are depicted in Figure 2. Process steps are color-coded: light shades indicate steps common to both routes, including raw material extraction at the raw material manufacturer, compounding at the material manufacturer, product use, and end-of-life treatment. Dark shades denote route-specific steps, namely the extrusion of the semi-finished plate stock versus filament extrusion at the material manufacturer, as well as material preparation and the respective bracket manufacturing process at the bracket manufacturer.

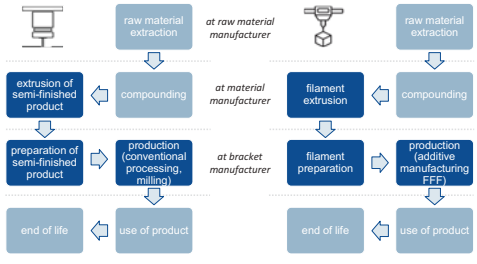

Fig. 2. Comparison of manufacturing routes for subtractive manufactured (with CNC milling) and additive manufactured (AM) brackets. Light shade: steps common to both routes; Dark shade: route- specific steps

4. Component Design

4.1. *Material selection and properties*

To meet the specified requirements, PA6-GF30 was selected as the structural material. It combines high strength, stiffness, and hardness with pronounced wear resistance, favorable sliding characteristics in contact with the component surface, and high damping capacity (Eyerer et al. (2005)). The incorporation of glass fibers enhances the

mechanical performance and reduces hydrophilicity; however, it also induces a more pronounced anisotropic material response, which is explicitly considered in the subsequent analyses.

The pre-processing steps for both product forms[a] are identical. For both materials – plate and filament – material data including stress-strain curves and flexural stress-strain curves from standardized tests are available. The filament-based specimens were produced – as intended for the application – using a miniFactory Ultra 3D Printing System with a heated build chamber, following drying and conditioning as described in Section 3, and employing comparable printing parameters. The corresponding mechanical tests were subsequently conducted under moisture-equilibrated conditions.

To quantify anisotropic properties, specimens were manufactured in different build orientations. The three orientation groups were chosen to capture the material response within the layer plane as well as along the build direction.

4.2. *Synthetic S-N curves*

Determining cyclic strength parameters by means of Wöhler (S-N) testing is already time- and resource-intensive; in the presence of anisotropy, the required experimental effort increases further due to directional dependence. According to Stommel et al. (2018), the ratio between cyclic and static strength for a given polymer type is approximately independent of the principal fiber orientation. This relationship is exploited here and combined with the experimentally determined failure data for the fatigue strength of PA-GF reported in Grellmann and Seidler (2024). A Basquin model (Stommel et al. (2018)) is fitted to the specimen failure data in log–log space and the associated scatter is estimated. Parameter estimation uncertainty is then propagated using parametric bootstrapping. For each bootstrap realization, the B_5 S–N curve is computed as the fifth percentile of the predicted life distribution as a function of stress amplitude. The B_5 S–N line at $90\,\%$ confidence is obtained as a pointwise one-sided lower confidence bound, i.e., the tenth percentile of the bootstrapped B_5 life estimates at each stress amplitude.

The S-N curves are assigned the experimentally determined material parameters of the plate stock for the machined bracket. Using the relation $\sigma_{zykl}(N)/\sigma_{stat} = \text{const.}$ from Stommel et al. (2018), dimensionless master S-N curves are derived, where σ_{stat} denotes the static strength, σ_{zykl} the cyclic strength, and N the crack-initiation cycle count. For the FFF-manufactured specimens, the S-N curves for different build orientations are obtained from the master S-N curves using the same relationship reverse. This yields direction-specific S-N curves for both manufacturing routes. The plate material exhibits substantially higher allowable pulsating stress amplitudes for the same target cycle counts. The properties along the build direction are, by a large margin, the least favorable. This can be attributed, first, to fiber orientations predominantly aligned within the layer plane and, second, to the reduced load-bearing capacity of the matrix bond caused by the sequential deposition of layers, which cannot be fully compensated even by a heated build chamber.

4.3. *Component design and strength verification*

The structural design of the CNC and AM brackets follows a three-stage procedure comprising preliminary sizing, static strength verification according to VDI 2016, and finite element analyses in ANSYS. The overall workflow, including inputs, intermediate results, and analysis branches, is summarized in Figure 3.

A preliminary sizing is performed using first-order Euler-Bernoulli beam theory. The maximum bending stress $\sigma_b = M_b/W_b$ at the maximum operating load $F_{max} = 138.1\,\mathrm{N}$ must remain below the allowable pulsating stress amplitude for a survival probability of $95\,\%$ at $10{,}000$ load cycles with a $90\,\%$ confidence level (Section 4.2). With a rectangular cross-section ($W_b = \frac{1}{6}\,b\,h^2$, $b = h$, Naefe and Luderich (2020)) and a cantilevered rigid beam loaded at $2/3$ of the leg length, a

[a]Plate stock (TECAMID 6 GF30 black) and filament (TECAFIL PA6 GF30 black) from Ensinger GmbH.

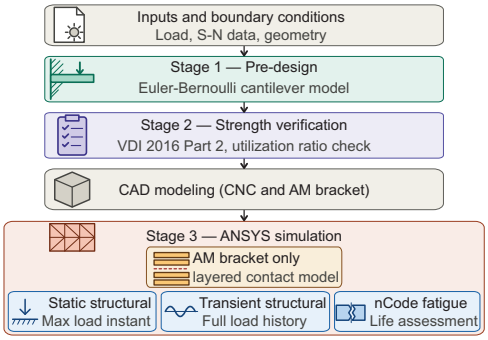

Fig. 3. Three-stage design and verification workflow for the CNC and AM brackets.

component height of $6.9\,\mathrm{mm}$ is required for the CNC bracket and $8.0\,\mathrm{mm}$ for the AM bracket.

The strength verification follows VDI 2016 Part 2 (Verein Deutscher Ingenieure (2025a)), which addresses unreinforced and short-fiber-reinforced thermoplastics. Direction-dependent stress-strain and flexural stress-strain curves (Section 4.2) provide the input; all strains remain below five percent, so no engineering-to-true strain conversion is required (Verein Deutscher Ingenieure (2025b)). Normalized initial moduli below five combined with repeated short-term loading yield the load factors, from which the component limit stresses are derived. A safety factor of 1.5 is applied to account for anisotropic material behavior. Using the allowable pulsating stress amplitudes as admissible equivalent stresses, material-specific utilization ratios below unity are obtained, confirming the preliminary sizing as the basis for CAD modeling.

Based on the CAD geometries, static structural analyses, transient structural analyses, and fatigue-life assessments using nCode are carried out in ANSYS. Static analyses are evaluated at the instant of maximum load (Figure 1), while transient analyses and nCode evaluations cover the complete load history. Direction-dependent material behavior is implemented as individually defined anisotropic parameter sets for strain- and stress-controlled S-N curves. For the AM bracket, the interlayer delamination mechanism is additionally investigated: the CAD model is discretized according to the slicing strategy of the print job, and the resulting 32 layers are coupled via contact interfaces (Figure 1).

5. Baseline Comparison

The bracket that is investigated is subject to mechanical stress during its period of use. In order to fulfill its function, this mechanical impact must be withstood. If the mechanical impact is not withstood, the bracket can no longer fulfill its function and must be replaced. This also has an impact on the ecological performance of the bracket. Therefore, it is essential to focus on the usage phase. A detailed examination of the usage phase was achieved with the help of reliability tests. Brackets for the same application are being investigated, but they undergo different production processes (AM vs. CNC). Both bracket geometries are similar, but not identical. They were designed to offer similar reliability, which resulted in slightly modified geometries and different masses of the bracket designs. In this case the AM bracket shows poorer mechanical characteristics. However, to compensate for this in terms of reliability, the geometry of the AM bracket has a larger cross-section.

The designs developed in Section 4 meet all assessed criteria regarding allowable displacements, strains, equivalent stresses, interlaminar displacements indicative of potential layer delamination, and the B_5 lifetime. The resulting required component thicknesses for the brackets are $6.9\,\mathrm{mm}$ (CNC) and $8.0\,\mathrm{mm}$ (AM). The corresponding masses of the finished brackets are $15\,\mathrm{g}$ (CNC) and $17.96\,\mathrm{g}$ (AM). For the AM bracket, an additional $2\,\mathrm{g}$ is included to account for the lead-in and lead-out material generated during printing. Since the plate stock used for CNC machining is only available in the next standard thickness of $8.0\,\mathrm{mm}$, this thickness is adopted for fabrication. Prior to processing, the $1.75\,\mathrm{mm}$ filament is dried in accordance with the manufacturer's specifications at $80\,^{\circ}\mathrm{C}$ for eight hours.

To quantify the GWP, a cradle-to-grave approach is selected as a system boundary, therefore all processes and phases in the life cycle of the brackets are taken into account. The functional unit of this investigation is defined as the production of one bracket with a defined reliability. To

assess the GWP of both product designs, primary data for the material consumption is used. Since both processes require the material in a differently processed form (filament for AM vs. plate stock for CNC), the processing of PA6-GF30 into filament or plate stock is modeled as shown in Figure 2 via literature data. The energy consumption of processes at the bracket manufacturer (plate stock preparation and conventional processing vs. filament preparation and FFF), as well as the end of life treatment, are also based on literature data.

The GWP results of the CNC and AM brackets are shown in Figure 4. The CNC bracket shows a GWP of $0.169\,\mathrm{kgCO_2-eq.}$. The material makes the largest contribution to GWP, accounting for $98.2\,\%$ of the total. For the AM bracket two scenarios are visualized – an opticstic and a conservative one. The difference between these two scenarios arises from uncertainties regarding energy consumption during the filament drying and chamber heating during the FFF process itself. The AM bracket shows a GWP of $0.281\,\mathrm{kgCO_2-eq.}$ (optimistic) and $0.570\,\mathrm{kgCO_2-eq.}$ (conservative). Compared to CNC, both AM-scenarios show a substantially higher total GWP and are therefore not competitive in this respect. While the GWP from the material is slightly lower, both scenarios suffer from a high GWP contribution from the process. For the optimistic the process contributes by $43.4\,\%$ whereas for the conservative it is $72.1\,\%$.

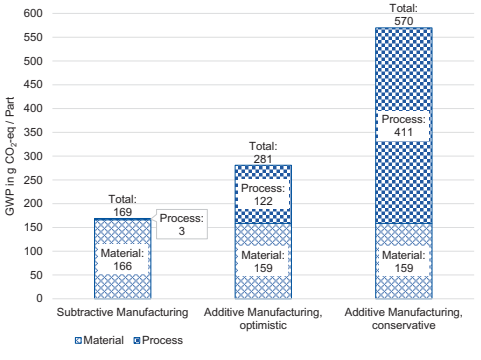

Fig. 4. GWP comparison of subtractive and additive manufactured brackets.

6. Optimization through Co-Design

For the CNC bracket, a reduction in component mass improves the material-related GWP only if it enables the use of smaller initial plate dimensions. Otherwise, mass reduction merely increases the amount of material removed during machining: while the GWP associated with producing the semi-finished stock remains unchanged, the process-related GWP increases due to additional manufacturing effort. This substantially limits the optimization potential of the CNC manufactured design; therefore, no further optimization is pursued under the given boundary conditions.

For the AM bracket, the situation differs fundamentally. Any reduction in filament consumption directly decreases the material-related GWP and, depending on process planning, may also indirectly reduce the process-related GWP through lower material throughput. Against this background, optimization measures are implemented for the AM manufactured design based on the functional requirements and the reliability assessment. Figure 5 compares the optimization variants with the CNC bracket and the AM baseline design for both conservative and optimistic scenarios.

First, the volume fill fraction of the rear mounting interface is optimized. Variant OF1 uses a reduced volume fill fraction of $60\,\%$, whereas variant OF2 applies an volume fill fraction of $20\,\%$ within the mounting volume of the bracket geometry. The resulting component masses are $13.55\,\mathrm{g}$ for OF1 and $12.08\,\mathrm{g}$ for OF2. For both variants, the GWP decreases markedly relative to the baseline; however, the difference between OF1 and OF2 remains comparatively small. The reduced infill is achieved by a combination of two measures, both of which are implemented in such a way that they do not affect the reliability of the bracket. Geometrically, pockets are introduced into the mounting interface. On process side, G-code is adapted within the slicing software to implement a lower infill density. The infill reduction is restricted to the mounting interface region, whereas the bracket legs remain designed as solid material to satisfy the mechanical requirements.

The second optimization targets a structural

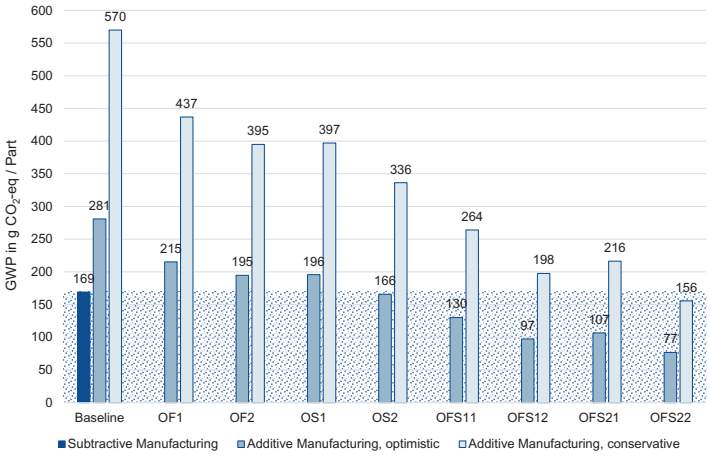

Fig. 5. Comparison of the baseline scenarios and different AM optimization variants (OF: Optimized Filling in mounting volume; OS: Optimized Structure of bracket legs; OFS: OF and OS combined).

modification of the bracket legs via topology optimization, which is depicted in Figure 6. This step leverages insights from the finite element analysis and the preliminary design. Material is selectively removed from regions of limited functional relevance while maintaining compliance with the static, dynamic, and fatigue requirements. An optimized design For OS1, the bracket mass is reduced by nearly $30\,\%$, whereas OS2 achieves a reduction slightly above $41\,\%$. While OS1 – similar to OF1 and OF2 – still exhibits a GWP slightly above that of the CNC bracket in the optimistic scenario, OS2 reaches a comparable GWP to the CNC bracket under optimistic assumptions.

Fig. 6. Structural optimized AM bracket design to fulfill the reliability requirements and reduce its GWP.

Variants OFS11, OFS12, OFS21, and OFS22 result from combining the optimized mounting-interface volume fill fraction (OF1, OF2) with the structurally optimized bracket legs (OS1, OS2). Combining OF1 and OS1 yields OFS11 with a mass of $8.25\,\mathrm{g}$. OFS22 represents the variant with the lowest filament usage, reducing filament consumption by more than $70\,\%$ relative to the baseline concept. Variants OFS12 and OFS21 yield intermediate GWP values between those four. Under optimistic assumptions, OFS11, OFS12, and OFS21 are expected to exhibit a lower GWP than the subtractively manufactured bracket; however, their conservative scenarios remain slightly above the reference value. Given the available information, it cannot be concluded unambiguously whether the CNC or AM variant yields a lower GWP for these cases. In contrast, the conclusion is clear for OFS22: both scenarios indicate a lower GWP than that of the CNC bracket.

All variants – from the baseline to OFS22 – satisfy the requirement of functional equivalence, yet exhibit substantial differences in GWP. The combination of reliability engineering and sustainability assessment enables a pronounced improvement in product performance for a design that initially appears non-competitive. In this manner, the co-design approach also reverses the conclusion regarding environmental sustainability when comparing the two manufacturing routes.

7. Conclusion

This paper demonstrates the potential for the co-design of reliability and environmental sustainability. It shows that credibly comparing manufacturing routes in terms of GWP requires functional equivalence anchored in an explicit reliability requirement rather than identical geometries.

For a dynamically loaded PA6-GF30 bracket, a simulation-based co-design of reliability and environmental sustainability is used to design, compare and optimize additive and subtractive manufacturing route under an equal-function constraint. The process-specific design takes the reliability requirements and the individual anisotropic material properties into account.

The scope of this comparison is limited to the investigated geometry class. For more complex parts, both routes are affected asymmetrically – AM through support structures for overhangs, CNC through multi-axis machining and higher chip-to-part ratios. The co-design framework itself remains applicable, but the direction and magnitude of the reliability-sustainability trade-off must be re-evaluated per geometry class.

In the baseline of the investigated bracket, CNC achieves much lower GWP than AM. For CNC from plate stock, upstream material provision of the plate stock dominates the impact. The GWP of the AM route is dependent on the raw material as well, but to a considerable extent also on the manufacturing process. Both factors depend heavily on the volume of filament used, and the design freedom offered by AM allows for substantial optimization potential. Optimized AM variants achieve substantial filament savings while maintaining reliability and can outperform CNC in GWP.

Acknowledgement

This work was supported by the German Research Foundation (DFG, Deutsche Forschungsgemeinschaft, Project-ID 279064222, Projects B03 and D02).

References

Bertsche, B. and M. Dazer (2022). *Zuverlässigkeit im Fahrzeug- und Maschinenbau: Ermittlung von Bauteil- und System-Zuverlässigkeiten* (4. Auflage ed.). Lehrbuch. Berlin and Heidelberg: Springer Vieweg.

Bongono, J., B. Elevli, and B. Laratte (2020). Functional unit for impact assessment in the mining sector—part 1. *Sustainability 12*(22), 9313.

Boothroyd, G., P. Dewhurst, and W. A. Knight (2010). *Product design for manufacture and assembly* (3rd ed. ed.), Volume 74 of *Manufacturing engineering and materials processing*. CRC Press.

European Commission (2021). COMMISSION RECOMMENDATION (EU) 2021/2279 of 15 December 2021 on the use of the Environmental Footprint methods to measure and communicate the life cycle environmental performance of products and organisations. *Official Journal of the European Union*.

Eyerer, P., P. Elsner, and T. Hirth (2005). *Die Kunststoffe und ihre Eigenschaften* (6., neu bearb. und erw. Aufl. ed.). VDI-Buch. Berlin and Heidelberg: Springer.

Grellmann, W. and S. Seidler (2024). *Kunststoffprüfung*. Carl Hanser Verlag GmbH Co KG.

International Organization for Standardization (2006a). ISO 14040 Environmental Management - Life Cycle Assessment - Principles and Framework.

International Organization for Standardization (2006b). ISO 14044 Environmental Management: Life Cycle Assessment ; Requirements and Guidelines.

Naefe, P. and J. Luderich (2020). *Konstruktionsmethodik für die Praxis: Aktuelle Verfahren in der Produktentwicklung* (2., überarbeitete Auflage ed.). Springer eBook Collection. Wiesbaden: Springer Vieweg.

Pérez, R., F. Argüelles, A. Laca, and A. Laca (2024). Evidencing the importance of the functional unit in comparative life cycle assessment of organic berry crops. *Environmental science and pollution research international 31*(14), 22055–22072.

Rockström, J., J. F. Donges, I. Fetzer, M. A. Martin, L. Wang-Erlandsson, and K. Richardson (2024). Planetary boundaries guide humanity's future on earth. *Nature Reviews Earth & Environment 5*(11), 773–788.

Stommel, M., M. Stojek, and W. Korte (2018). *FEM zur Berechnung von Kunststoff-und Elastomerbauteilen*. Carl Hanser Verlag GmbH Co KG.

Verein Deutscher Ingenieure (2025a, 09). Festigkeitsnachweis von Bauteilen aus thermoplastischen Kunststoffen - Festigkeitsnachweis gegenüber statischen Belastungen. VDI-Richtlinie VDI 2016 Blatt 2. Hrsg. Verein Deutscher Ingenieure (VDI).

Verein Deutscher Ingenieure (2025b, 09). Festigkeitsnachweis von Bauteilen aus thermoplastischen Kunststoffen - Grundlagen. VDI-Richtlinie VDI 2016 Blatt 1. Hrsg. Verein Deutscher Ingenieure (VDI).